# Performance Evaluation of SiPM Detectors for PET Imaging in the Presence of Magnetic Fields

Samuel España, *Student Member, IEEE*, Gustavo Tapias, Luis M. Fraile, Joaquín L. Herraiz, *Student Member, IEEE*, Esther Vicente, *Student Member, IEEE*, Jose Udias, *Member, IEEE*, Manuel Desco, Juan J. Vaquero, *Senior Member, IEEE*

***Abstract*– The multi-pixel photon counter (MPPC) or silicon photo-multiplier (SiPM), recently introduced as a solid-state photodetector, consists of an array of Geiger-mode photodiodes (microcells). It is a promising device for PET thanks to its potential for high photon detection efficiency (PDE) and immunity to high magnetic fields. It is also very easy to use, with simple electronic read-out, high gain and small size. In this work we evaluate the performance of three 1 × 1 mm$^2$ and one 6 × 6 mm$^2$ (2 × 2 array) SiPMs offered by Hamamatsu for their use in PET. We examine the dependence of the energy resolution and the gain of these devices on the thermal and reverse bias when coupled to LYSO scintillator crystals. We find that the 400 and 1600 microcells models and the 2 × 2 array are suitable for small size crystals, like those employed in high resolution small animal scanners. The good performance of these devices up to 7 Tesla has also been confirmed.**

## I. Introduction

POSITRON emission tomography (PET) scanners have been used to investigate biochemical and pathological phenomena, to diagnose disease, and to determine prognosis after treatment. On the other hand, magnetic resonance imaging (MRI) provides unsurpassed soft-tissue contrast and does not require the use of ionizing radiation. Therefore, it is expected that combined PET/MR scanners represent the future for biomedical imaging [1], and that these scanners will either supplement or compete with PET/CT for basic research and clinical applications. However, one major obstacle of the combined PET/MR system with photomultiplier tubes (PMT) is that these tubes are extremely sensitive to magnetic fields.

PET/MR using PMTs involves the use of long optical fibers to transfer the light signals from the scintillation crystals located inside the MR scanner [2]. This method produces a degradation of energy resolution due to light losses during the optical transfer.

The use of semiconductor photo-detectors, such as avalanche photodiodes (APD) instead of PMTs offers an alternative development option which is currently being pursued by several research groups [3]. APDs are compact and insensitive to magnetic fields as compared with PMTs, and these properties are desirable for PET/MR. One disadvantage of presently available APDs is that they have low gains of an order of a few hundreds, and thus require sophisticated preamplifiers.

New alternatives for PET/MR scanners are Silicon Photomultiplier detectors (SiPM). These devices are solid-state photodetectors consisting of an array of photodiodes (microcells) operated in Geiger mode [4]. They exhibit good photon detection efficiency (PDE) and they should not be affected by external magnetic fields. They are easy to use, require simple electronics, do not need high voltage power supplies and provide a high gain, all in a compact size. Their insensitivity to magnetic field makes them suitable for development of PET scanners for simultaneous PET/MR studies. Several groups are studying the SiPM performance for PET purpose showing promising results [5, 6].

## II. Materials and Methods

In this work we evaluate three 1 × 1 mm$^2$ SiPM models with 100, 400 and 1600 microcells and a 6 × 6 mm$^2$ (2 × 2 array) SiPM with 3600 microcells per element , all of them from Hamamatsu, for their use in PET and PET/MR. They were coupled to 1.5 × 1.5 × 12 mm$^3$ LYSO crystals. We have studied the performance of these devices and their immunity to magnetic fields of up to 7 Tesla with superconducting magnet from Bruker.

TABLE I
SiPM USED ON THE PRESENT STUDY

| Series | Active area (mm2) | Number of microcells | Pixel size (μm) | Fill factor | P.D.E. (%) |
|---|---|---|---|---|---|
| S10362-11-100P | 1 × 1 | 100 | 100 | 78.5 | 75 |
| S10362-11-050P | 1 × 1 | 400 | 50 | 61.5 | 50 |
| S10362-11-025P | 1 × 1 | 1600 | 25 | 30.8 | 25 |
| MPPC-33-2x2-50 5900 | 6 × 6 (2 × 2 array) | 3600/ element | 50 | 61.5 | 50 |

Data acquisition was performed using an Agilent 6000 series oscilloscope (2 GSa/s). The oscilloscope was placed in the MRI controller room using 5 m long cables for the output

Manuscript received November 14, 2008. This work was supported in part by the MEC (FPA2007-07393), CDTEAM (CENIT-Ingenio 2010) Ministerio de Industria, Spain, UCM (Grupos UCM; 910059), CPAN (Consolider-Ingenio 2010) CSPD-2007-00042 projects, and the RECAVA-RETIC network.

S. España, L. M. Fraile, J. L. Herraiz, E. Vicente and J. M. Udías are with the Grupo de Física Nuclear, Dpto. Física Atómica, Molecular y Nuclear, Universidad Complutense de Madrid, Spain (S. España email: samuel@nuclear.fis.ucm.es).

G. Tapias, M. Desco and J. J. Vaquero are with the Unidad de Medicina y Cirugía Experimental, Hospital General Universitario Gregorio Marañón, Madrid, Spain (J. J. Vaquero email: juanjo@mce.hggm.es).

signals. The power supply for the SiPM and the amplifier circuit was placed in the MR scanning room behind the 5 Gauss line and were connected by 2 m long cables.

### *A. Single SiPM*

Fig. 1 shows the experimental setup employed for the 1 × 1 $mm^2$ SiPMs. Each SiPM is coupled with optical grease to a LYSO crystal wrapped with Teflon. A Delrin case was used to prevent external light from reaching the SiPM.

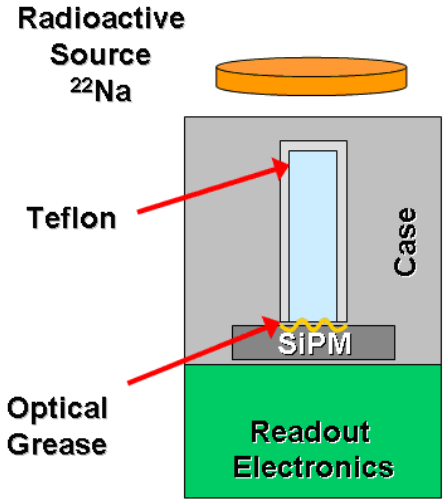


Fig. 1. Experimental setup used for 1 × 1 $mm^2$ SiPM.

fast shaper, providing pulses with 100 ns width, has been designed and constructed for the readout of the SiPMs (see Fig. 2). This allows for very high counting rates to be handled.

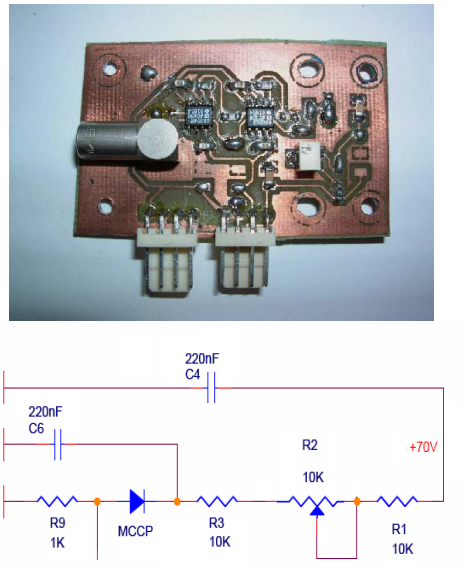


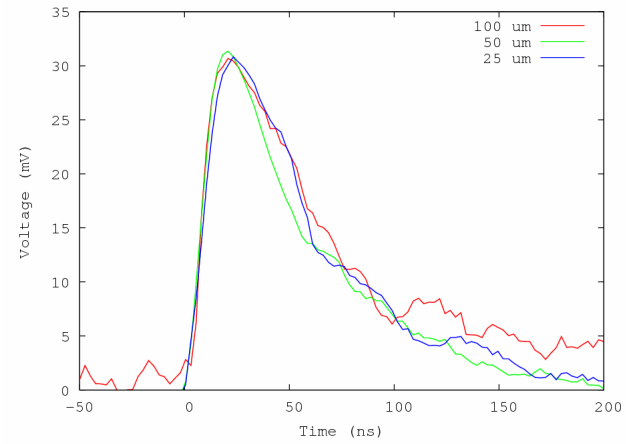


Fig. 2. Picture (top) and scheme (middle) of the readout electronics built for the 1 × 1 $mm^2$ SiPMs. Pulses obtained from the single SiPMs with different pixel size (bottom).

We have measured the energy resolution of these devices, and the dependence of the gain with reverse bias and temperature with a 22Na radioactive source in the presence of magnetic fields of 0 and 7 T.

### *B. SiPM array*

A 4 × 4 LYSO crystal matrix was coupled to the 2 × 2 SiPM array. Each crystal element, individually wrapped in Teflon, has a size of 1.5 × 1.5 × 12 $mm^3$ (see Fig. 3), wrapped individually with Teflon.

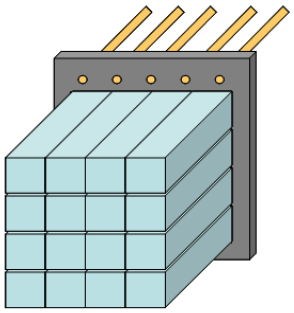

Fig. 3. Experimental setup used for SiPM array.

Readout electronics, specifically tailored to this application was built in order to acquire the signals from the SiPM channels as well as an additional signal with the sum of all channels, which is used as external trigger.

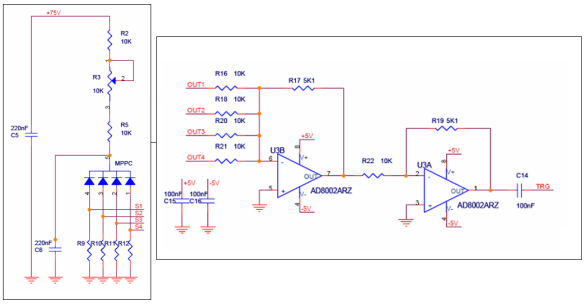

Fig. 4. Scheme of the electronics readout used for the SiPM array.

The energy resolution and flood histogram were measured for both 0 and 7 Tesla. A $^{18}$F radioactive source was used for these measurements.

## III. Results

### A. Single SiPM

Fig. 5 shows the energy spectra obtained for the three 1 × 1 mm$^2$ SiPMs using a $^{22}$Na radioactive source. They must be linearized since the SiPMs saturate when most of the pixels are triggered. The 511 keV peak is clearly resolved in all cases but the 1.275 MeV peak is not so well resolved due to saturation. Obviously the higher the number of microcells the less the saturation and therefore the 1275 keV peak is better observed for the SiPM with 1600 microcells.

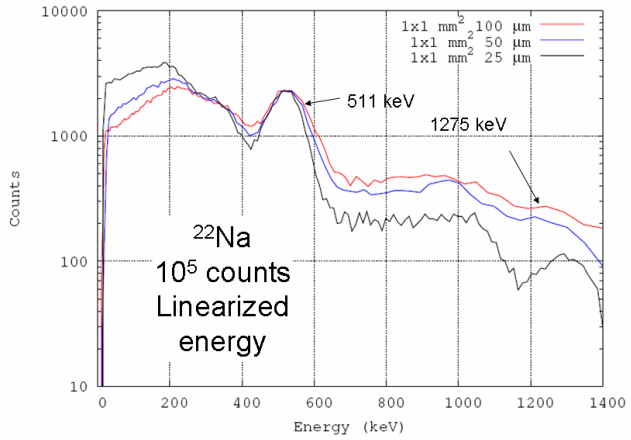


Fig. 5. Energy spectra obtained for the three single SiPMs using a $^{22}$Na radioactive source.

The energy resolution at 511 keV is shown in Fig. 6 as the percentage FWHM of the peak, as a function of applied voltage. The best FWHM was obtained for he SiPMs with 1600 and 400 microcells. Furthermore, the 1600 microcells FWHM does not change with voltage. Red lines are the results at 0 Tesla measurement and green lines are for those at 7 Tesla. Both measurements were performed at the same temperature of 20ºC and yield very similar results.

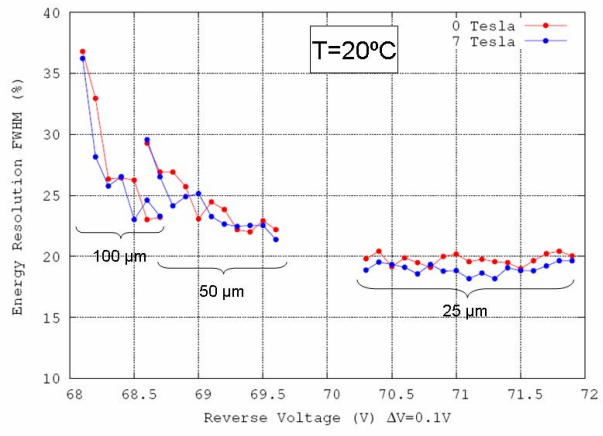


Fig. 6. Energy resolution as a function of voltage.

In Fig. 7, the relative gains for the same measurements shown in Fig. 6 are graphed. The slope is smaller for the SiPM with 1600 microcells followed by those with 400 and 100 microcells. The slopes are comparable for the 0 and 7 Tesla measurements.

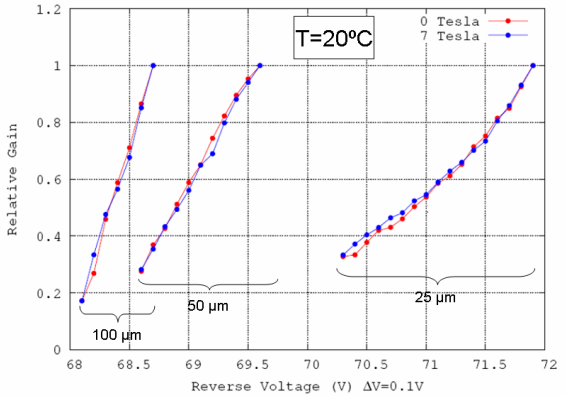


Fig. 7. Relative gain as a function of voltage.

The energy resolution at 511 keV was also measured for a fixed voltage for each SiPM as a function of temperature. The SiPMs with 1600 and 400 microcells exhibit again the most stable behavior compared with the 100 microcells SiPM (see Fig. 8).

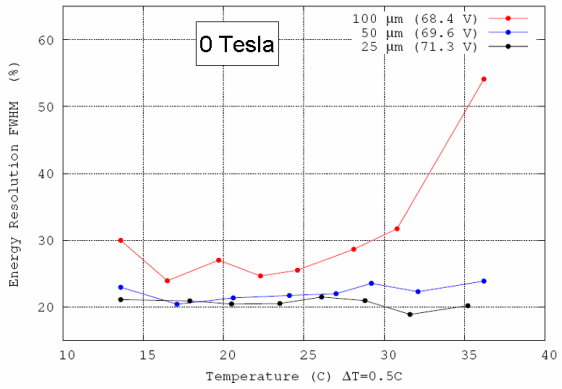


Fig. 8. Energy resolution as a function of temperature.

The variation of the relative gain as a function of the temperature shows once again more uniform behavior of the 40 and 1600 microcells SiPMs (see Fig. 9).

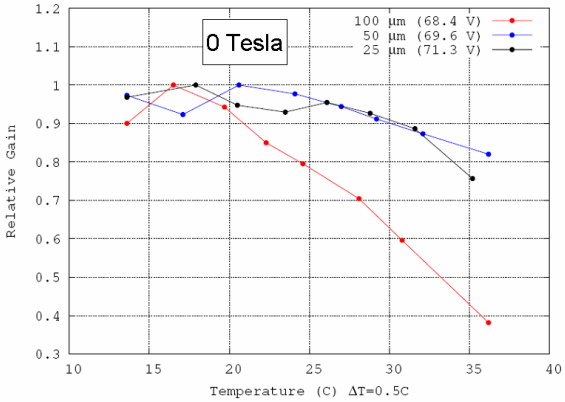


Fig. 9. Relative gain as a function of temperature.

$$\text{Gain Variation} = \frac{\Delta Gain/\Delta Voltage}{Gain} \cdot 100 \ (\%\cdot V^{-1}) \quad (1)$$

Table II shows the gain variation (see eq. 1) with voltage and with temperature as a summary of the results obtained with the single SiPMs. The variation is smaller for the 400 and 1600 microcells SiPMs.

TABLE II
SUMMARY OF RESULTS FOR SINGLE SIPM BY MEANS OF GAIN VARIATION

| Gain Variation | 0 Tesla *7 Tesla* | Constant T | Constant V |
|---|---|---|---|
| 100 microcells | 230 %·V-1 *235 %·V-1* | -2.7 %·ºC-1 | |
| 400 microcells | 110 %·V-1 *110 %·V-1* | -0.4 %·ºC-1 | |
| 1600 microcells | 70 %·V-1 *75 %·V-1* | -1.1 %·ºC-1 | |

*B. SiPM array*

Fig. 10 shows the four channel signals of an event. The total width of the pulses is about 200 ns and the height is a few hundreds mV. These pulses are integrated and Anger logic is employed to compute the centroid of the interactions.

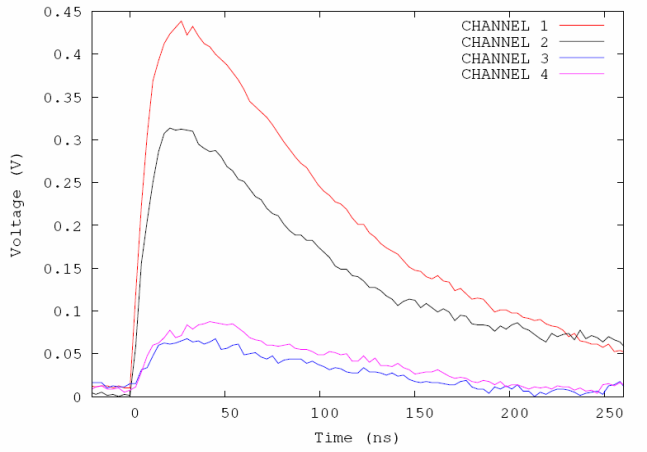


Fig. 10. Pulses of four channels for one event detected with the SiPM array.

The flood histogram shown in Fig. 11 was obtained in an acquisition of 5 minutes with a $^{18}$F source, accumulating $5{\cdot}10^5$ counts. All the crystals of the matrix are clearly resolved.

On the same figure, the horizontal profile of counts inside the red rectangle of the flood histogram is shown. Red and green lines of the figure represent the results obtained for 0 and 7 Tesla measurements respectively showing the same results. A fixed value of the bias voltage of 68.2 V was applied, while the temperature was kept at 20ºC. A peak to valley ratio of 10:1 is achieved.

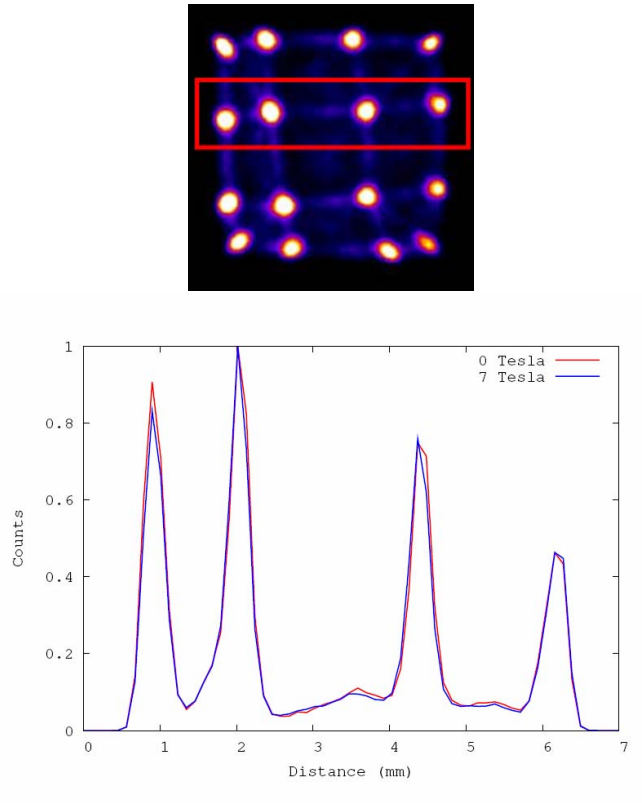


Fig. 11. Flood histogram (top) and horizontal line profile (bottom).

Energy spectra for every crystal element measured at 0 and 7 Tesla are shown in Fig. 12. The differences for the results with and without magnetic field are negligible. An additional acquisition was performed using a $^{22}$Na in order to test the linearity of the energy spectrum. Fig. 12 (bottom) shows the good linearity for the energy spectrum obtained with a single crystal placed at the center of the matrix.

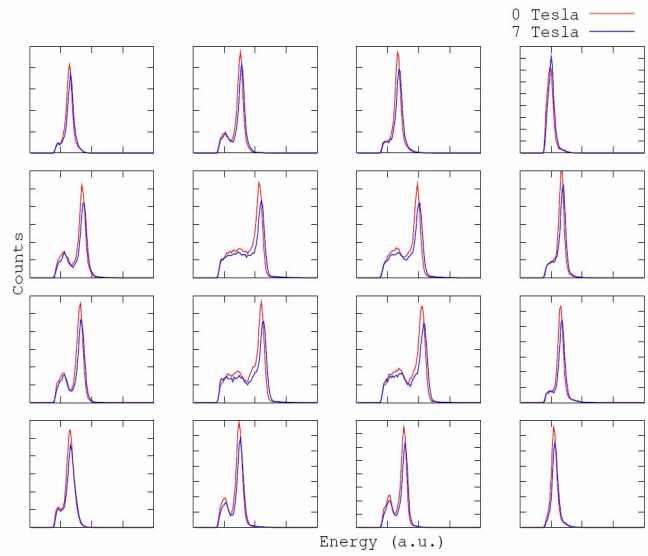

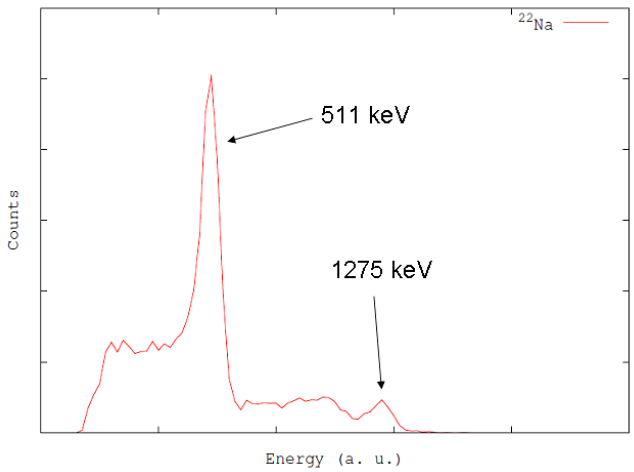


Fig. 12. Energy spectra obtained for each crystal element using $^{18}$F (top) and for one crystal at the center of the matrix using $^{22}$Na.

The energy resolution at 511 keV for sample crystals placed at different location inside the matrix is shown in table III.

TABLE III
ENERGY RESOLUTION FOR CRYSTAL ELEMENT AT DIFFERENT POSITIONS INSIDE THE MATRIX

| FWHM (%) | 0 Tesla | 7 Tesla |
|---|---|---|
| Center | 11.2 | 11.9 |
| Center edge row | 14.1 | 14.4 |
| Corner | 21.7 | 21.4 |

## IV. CONCLUSIONS

Single SiPMs with an active area of 1 × 1 mm2 have been tested at 0 and 7 Tesla. We found no significant magnetic field effect. The 400 and 1600 microcells SiPMs seem more suitable for PET purposes exhibiting better and more stable energy resolution. A 2 × 2 SiPM array has also been examined in conjunction with a 4 × 4 LYSO crystal matrix. All the 4 × 4 crystals of 1.5 mm pitch size were perfectly resolved by the 2 × 2 SiPM array, yielding a 10:1 peak to valley ratio in the counts profile at both 0 and 7 Tesla. Our measurements show the strong potential for PET/MR scanners with scintillator crystal sizes of 1 mm.

## ACKNOWLEDGMENT

Part of the computations of this work were done at the “High Capacity Cluster for Physical Techniques" of the Faculty for Physical Sciences of the UCM, funded in part by the UE under the FEDER program and in part by the UCM. E. Vicente acknowledges support from CSIC-JAE predoctoral fellowships respectively.

## REFERENCES

[1] Gaa, J., E.J. Rummeny, and M.D. Seemann, *Whole-body imaging with PET/MRI.* Eur. J. Med. Res., 2004. **9**: p. 309-12.
[2] Shao, Y., et al., *Simultaneous PET and MR imaging.* Phys Med Biol, 1997. **42**: p. 1965-70.
[3] Pichler, B., et al. *Performance Test of a LSO-APD PET Module in a 9.4 Tesla Magnet*. in *IEEE NSS-MIC*. 1998.
[4] Renker, D., *Geiger-mode avalanche photodiodes, history, properties and problems.* Nucl. Inst. Meth. In Phy. Res. A, 2006. **567**: p. 48-56.
[5] Otte, A.N., et al., *A test of Silicon Photomultipliers as readout for PET.* Nucl. Inst. Meth. In Phy. Res. A, 2005. **545**(3): p. 705-15.
[6] Llosá, G., et al. *Silicon Photomultipliers and SiPM matrices as Photodetectors in Nuclear Medicine*. in *IEEE NSS-MIC*. 2007.